

Water quality and aquatic ecology modelling suite

D-WATER QUALITY

Deltares systems

SWITCH

SWITCH

Prediction of the nutrient fluxes across the sediment-water interface

Technical Reference Manual

D-Water Quality

Version: 4.00
Revision: 78574

23 September 2023

SWITCH, Technical Reference Manual

DRAFT

Published and printed by:

Deltares
Boussinesqweg 1
2629 HV Delft
P.O. 177
2600 MH Delft
The Netherlands

telephone: +31 88 335 82 73

e-mail: [Information](#)

www: [Deltares](#)

For sales contact:

telephone: +31 88 335 81 88

e-mail: [Sales](#)

www: [Sales & Support](#)

For support contact:

telephone: +31 88 335 81 00

e-mail: [Support](#)

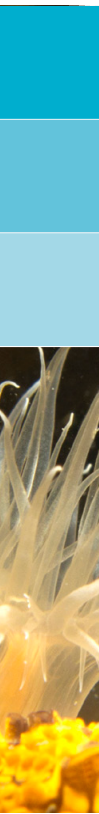
www: [Sales & Support](#)

Copyright © 2023 Deltares

All rights reserved. No part of this document may be reproduced in any form by print, photo print, photo copy, microfilm or any other means, without written permission from the publisher: Deltares.

Contents

List of Tables	v
List of Figures	vii
1 Introduction	1
2 Spatial schematisation and processes	3
3 Aerobic layer and the sediment oxygen demand	9
4 Denitrifying layer and nitrate	11
5 Detritus	13
6 Ammonium	17
7 Phosphate	19
8 Silicate	25
9 Temperature dependency and dispersion	27
References	29

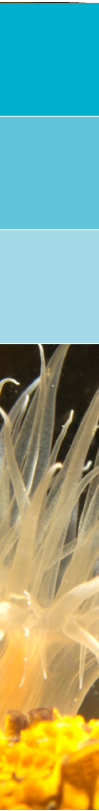


DRAFT

List of Tables

2.1	Initialisation parameters for SWITCH	4
2.1	Initialisation parameters for SWITCH	5
2.2	Numerical input parameters for SWITCH	5
2.2	Numerical input parameters for SWITCH	6
2.3	Physical input parameters for SWITCH	6
2.3	Physical input parameters for SWITCH	7
2.4	(Bio)chemical input parameters for SWITCH	7
2.4	(Bio)chemical input parameters for SWITCH	8

DRAFT

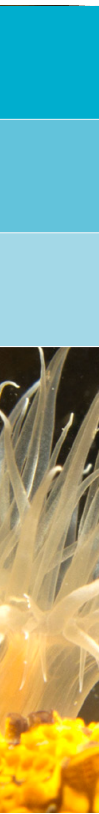


DRAFT

List of Figures

2.1	Schematisation of the sediment layer in SWITCH	3
2.2	Overview of the processes included in SWITCH	4

DRAFT



DRAFT

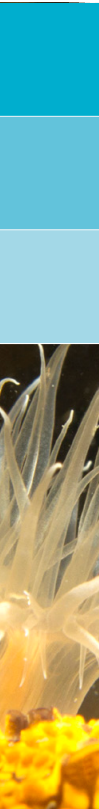
1 Introduction

SWITCH was made as a sub-model of the surface water eutrophication model DBS for the prediction of the nutrient fluxes across the sediment-water interface (WL | Delft Hydraulics, 1992). The acronym stands for Sediment Water Interaction by Transport and Chemistry. SWITCH distinguishes four sediment layers and calculates the thicknesses of the aerobic and denitrifying layers on the basis of a steady state approach. The concentrations of detritus, ammonium, nitrate, phosphate and silicate in the sediment and the pore water are simulated dynamically using mass balance equations.

SWITCH is applied as part of the eutrophication models, specific configurations of DELWAQ among which DBS and GEM. The link between these models and sub-model SWITCH is formed by the sediment-water exchange fluxes of dissolved oxygen, nutrients and organic matter. SWITCH acts directly on substances in the water column, just like any other process routine in DELWAQ. Specific facilities have been developed for the coupling of SWITCH to DELWAQ. These include a fractional step numerical computation procedure and an sediment-water aggregation procedure. The fractional step procedure takes care that SWITCH operates according to an appropriate computational time step, equal to or smaller than the DELWAQ time step, in order to maintain computational stability at steep concentration gradients and large mass fluxes between water and sediment. The sediment-water aggregation procedure allows the aggregation of several water segments with respect to SWITCH in order to establish a reduction of the computational burden. This means that the exchange of substances with the sediment underlying such a group of water segments is computed by SWITCH in one stroke. Both procedures are described in the process documentation regarding SWITCH in Chapter 8 of this manual.

Details with respect to background, objectives, starting-points and formulations of SWITCH have been described in WL | Delft Hydraulics (1994b,c). The first version of SWITCH and the first application for Lake Veluwe, the sediment of which is a mixture of silt and sand, have also been described by Smits and Van der Molen (1993). Other applications of SWITCH concerned the Lake Volkerak-Zoommeer (WL | Delft Hydraulics, 1995), with deep gullies and silty sediment, the peat lakes Geerplas and Nanneveld (WL | Delft Hydraulics, 1997) and the sandy coastal strip of the North Sea.

Volume units refer to bulk (ℓ) or to water (w).



DRAFT

2 Spatial schematisation and processes

Figure 2.1 depicts the vertical schematisation of the 'active' sediment layer in SWITCH. An overview of the processes included in SWITCH is given in Figure 2.2. The 'active' sediment layer has a constant thickness (d), and is divided in 4 sub-layers. An upper layer (d_h) and a lower layer ($d_l=d_4$) have been defined in order to account for vertical characteristics such as decomposition of organic matter, dispersion and porosity. These layers are also fixed. A second partition follows from chemical differences. A thin top layer (d_o) is oxidising, the remaining part ($d_h-d_o = d_3$, $>$ minimal value) of the upper layer is reducing. The oxidising layer is divided in an oxygen containing layer d_1 and a denitrifying layer d_2 . Both d_1 and d_2 are variable, and are deduced from steady-state solutions of the mass balance equations for dissolved oxygen and nitrate. In order to avoid numerical problems neither d_o nor d_1 may become infinitely thin, a minimal thickness ($d_{1,m}$) has therefore been defined. However, the denitrifying layer disappears entirely, when the nitrate concentration drops below a critical value ($C_{n,c}$).

Additionally, a very thin meta-stable boundary layer has been defined, which contains the detritus settled from the overlying water (and produced from microphytobenthos). From this layer detritus is incorporated in the sediment as the consequence of bioturbation. Nutrients produced from decomposition of detritus in the boundary layer are allocated to the oxygen containing top layer. The same goes for the dissolved oxygen fluxes pertaining to these processes. The boundary layer as such may affect the dispersion of dissolved substances across the sediment-water interface, which can be taken into account in SWITCH.

Table 2.1 upto Table 2.4 present an overview of the input parameters for SWITCH. In addition SWITCH needs mass fluxes from the water column connected with the settling of particulate substances and the dissolved concentrations in the water column for the calculation of diffusive exchange and downwelling seepage.

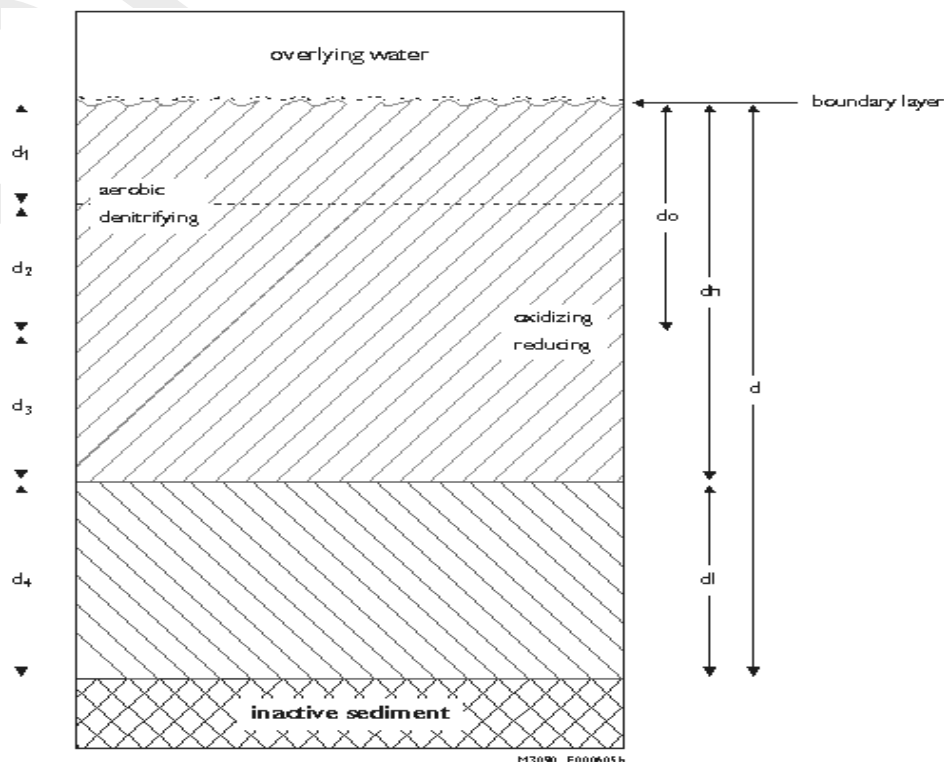


Figure 2.1: Schematisation of the sediment layer in SWITCH

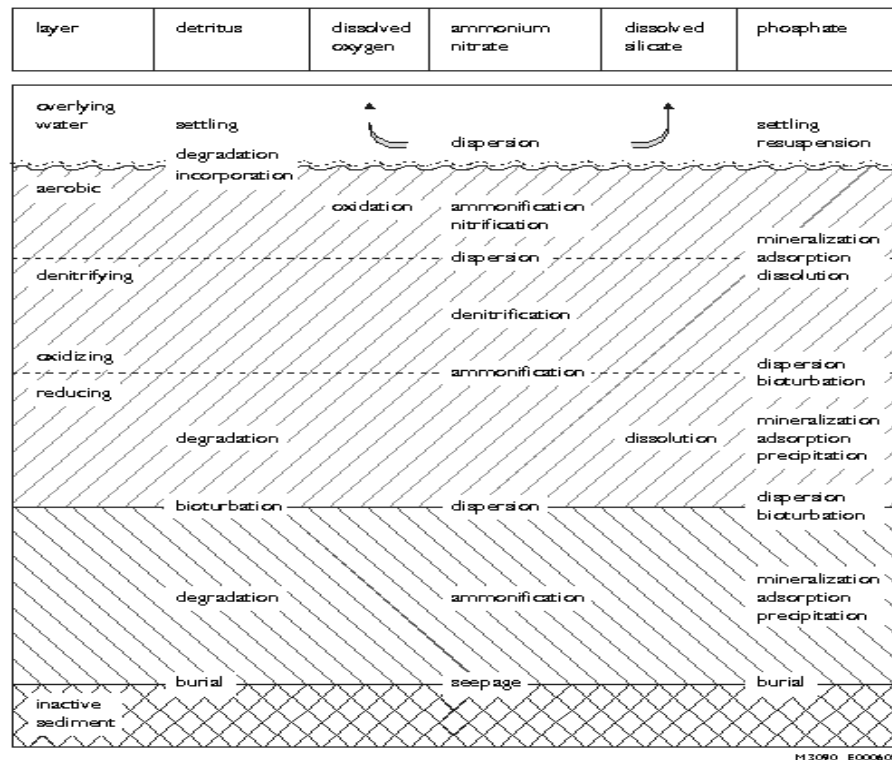


Figure 2.2: Overview of the processes included in SWITCH

As mentioned in the introduction SWITCH is applied as part of the eutrophication models, specific configurations of DELWAQ among which DBS and GEM. In this setting the meta-stable boundary layer is modelled as the S1 sediment layer, which contains so-called “inactive substances” such as detritus and benthic algae, together shaping up the benthic complex. (However, benthic algae may be excluded from the simulation). All nutrient fluxes inferred by the algae are accounted for, either directly in the boundary layer (S1) or in the upper sediment layer 1 in SWITCH. Algae are incorporated from the boundary layer into the sediment in exactly the same way as detritus, which is taken care of by the process called “burial”. The way settling particulate matter is added to boundary layer S1 or directly to the upper sediment layer 1 is described in the process description in Chapter 8 of this manual.

Table 2.1: Initialisation parameters for SWITCH

Parameter	Symbol in appendix	Value (indicative)	Units
<u>Dissolved substances</u>			
Nitrate:			
Layer 1	Cn ₁	1.0	gN m _w ⁻³
Ammonium:			
Layer 1:	Ca ₁	1.5	gN m _w ⁻³
Layer 2–3:	Ca ₂	3.0	gN m _w ⁻³
Layer 4:	Ca ₄	4.0	gN m _w ⁻³
Silicate:			
Layer 1–1:	Cs ₁	8.0	gSi m _w ⁻³

Table 2.1: Initialisation parameters for SWITCH

Parameter	Symbol in appendix	Value (indicative)	Units
<u>Partitioned substances</u>			
Total inorganic phosphate content:			
Layer 1–2:	Cp ₁	140.0	gP m _ℓ ⁻³
Layer 3:	Cp ₃	105.0	gP m _ℓ ⁻³
Layer 4:	Cp ₄	84.0	gP m _ℓ ⁻³
Fraction of phosphate in vivianite:			
Layer 1–2:	fpp ₁	0.1	-
Layer 3:	fpp ₃	0.3	-
Layer 4:	fpp ₄	0.5	-
Fraction of phosphate in stable mineral:			
Layer 1–2:	fmp ₁	0.4	-
Layer 3:	fmp ₃	0.4	-
Layer 4:	fmp ₄	0.4	-
<u>Particulate substances</u>			
Detritus content in the upper layer 1–3			
Carbon	Cd ₁	700.0	gC m _ℓ ⁻³
Nitrogen	Cnd ₁	40.0	gN m _ℓ ⁻³
Phosphorus	Cpd ₁	3.5	gP m _ℓ ⁻³
Detritus content in the lower layer 4			
Carbon	Cd ₄	160.0	gC m _ℓ ⁻³
Nitrogen	Cnd ₄	7.0	gN m _ℓ ⁻³
Phosphorus	Cpd ₄	0.7	gP m _ℓ ⁻³
Refractory detritus content in layer 1–4			
Carbon	Cr _{d1}	0.0	gC m _ℓ ⁻³
Nitrogen	Cr _{n1}	0.0	gN m _ℓ ⁻³
Phosphorus	Cr _{p1}	0.0	gP m _ℓ ⁻³

Table 2.2: Numerical input parameters for SWITCH

Parameter	Symbol in appendix	Value	Units
Minimal thickness (depth) of the aerobic layer 1	d _{1m}	0.0005	m
Crit. thickness layer 1 for obt. red. sorp. capacity	do _m	0.0009	m

Table 2.2: Numerical input parameters for SWITCH

Parameter	Symbol in appendix	Value	Units
Crit. (=max) nitrate conc. for sulphate reduction	Cn_c	0.05	$gN\ m^{-3}$

Table 2.3: Physical input parameters for SWITCH

Parameter	Symbol in appendix	Value	Units
<u>The sediment</u>			
Thickness (depth) of the aerobic top layer 1 ¹⁾	d_1	0.001	m
Thickness (depth) of the denitrifying layer 2 ¹⁾	d_2	0.004	m
Thickness (depth) of the upper reducing layer 3 ¹⁾	d_3	0.015	m
Thickness (depth) of the lower reducing layer 4	$d_4 = dl$	0.08	m
Thickness (mixing length) of the water boundary layer	l	0.001	m
Porosity of the upper layer	p_1	0.75	$m_w^3\ m_b^{-3}$
Porosity of the lower layer	p_4	0.65	$m_w^3\ m_b^{-3}$
Specific weight (density) of dry matter	Ws	2400.0	$kg\ m^{-3}$
<u>Mass transport</u>			
Seepage (- downwelling or + upwelling)	vs	0.0	m/day
Ammonium conc. at lower boundary in upw. water	Ca_5	4.0	$gN\ m_w^{-3}$
Phosphate conc. at lower boundary in upwelling water	Cdp_5	0.05	$gP\ m_w^{-3}$
Silicate conc. at lower boundary in upwelling water	Cs_5	10.0	$gSi\ m_w^{-3}$
Sedimentation rate (gross sediment accretion rate)	Fs	0.0	$\frac{m_b^3\ m^{-2}}{d^{-1}}$
Resuspension rate	Fr	0.0	$\frac{m_b^3\ m^{-2}}{d^{-1}}$
Fraction of surface area closed by the benthic complex	fc	0.0	-
Molecular diffusion coefficient oxygen	Dm_o	$5.5 \cdot 10^{-5}$	$m^2\ d^{-1}$
Molecular diffusion coefficient ammonium	Dm_a	9.0 „	$m^2\ d^{-1}$
Molecular diffusion coefficient nitrate	Dm_n	9.3	$m^2\ d^{-1}$
Molecular diffusion coefficient phosphate	Dm_p	4.2 „	$m^2\ d^{-1}$
Molecular diffusion coefficient silicate	Dm_s	4.7 „	$m^2\ d^{-1}$
Bio-irrigation multiplication factor;			

Table 2.3: Physical input parameters for SWITCH

Parameter	Symbol in appendix	Value	Units	
mean	bt	3.0	-	
amplitude		2.0	-	
period		365	d	
phase		0.2	-	
Bioturbation dispersion coefficient;		Db		
mean			$1.0 \cdot 10^{-6}$	$m^2 d^{-1}$
amplitude			$1.0 \cdot 10^{-6}$	$m^2 d^{-1}$
period			365	d
phase			0.2	-

¹⁾ d_1 , d_2 and d_3 shape up the upper layer d_h , which is constant in thickness just as $d_l (=d_4)$.

Table 2.4: (Bio)chemical input parameters for SWITCH

Parameter	Symbol in appendix	Value	Units
<u>Detritus</u>			
Incorp. rate from bound. layer into up. layer at 20 °C ¹⁾	rc^{20}	0.04	d^{-1}
Temperature coefficient for incorporation*	k _{ti}	1.07	-
Mineralisation rate in the boundary layer at 20 °C ²⁾	kc_b^{20}	0.075	d^{-1}
Mineralisation rate in the upper layer at 20 °C	kc_1^{20}	0.055	d^{-1}
Mineralisation rate in the lower layer at 20 °C	kc_4^{20}	0.0065	d^{-1}
Temperature coefficient for mineralisation	k _{tc}	1.07	-
Add. frac. detritus turned into refractory org. matter	frf	1.0	-
<u>Ammonium and Nitrate</u>			
Nitrification rate	kn^{20}	50.0	d^{-1}
Temperature coefficient for nitrification	k _{tn}	1.07	-
Denitrification rate at 20 °C	kd^{20}	50.0	d^{-1}
Temperature coefficient for denitrification	k _{td}	1.07	-
Stoich. constant for nitrogen in refractory org. matter	aa	0.04	$gN gC^{-1}$
<u>Phosphate</u>			
Adsorption capacity of oxidising layer 1-2	Cac_o	0.8	$gP kgDM^{-1}$

Table 2.4: (Bio)chemical input parameters for SWITCH

Parameter	Symbol in appendix	Value	Units
Adsorption capacity of upper reducing layer 3	Cac_r	0.4 or -999	$gP \text{ kgDM}^{-1}$
Half saturation constant for adsorption at 20 °C	Ks^{20}	0.1	$gP \text{ m}_w^{-3}$
Temperature coefficient for half saturation constant	kta	1.0	-
Precipitation rate at 20 °C	kp^{20}	0.8	d^{-1}
Fraction precipitated phosphate into the stable mineral	fm	0.0	-
Saturation concentration for precipitation	Cdp_s	0.05	$gP \text{ m}_w^{-3}$
Temperature coefficient for precipitation	ktp	1.0	-
Dissolution / oxidation rate of vivianite at 20 °C	kdp^{20}	0.01	$m^{-2.01} gP^{0.67} d^{-1}$
Temperature coefficient for dissolution	$ktdp$	1.0	-
Stoich. constant for phosphorus in refract. org. matter	ap	0.004	$gP \text{ gC}^{-1}$
<u>Silicate</u>			
Dissolution rate of opal silicate at 20 °C	ks^{20}	0.09	d^{-1}
Saturation concentration for dissolution	Cs_s	10.0	$gSi \text{ m}_w^{-3}$
Temperature coefficient for dissolution	kts	1.0	-
<u>Oxygen</u>			
Stoich. constant for consump. at mineralis. of detritus	ac	3.1	$gO_2 \text{ gC}^{-1}$
Stoich. constant for consump. at nitrification	an	4.57	$gO_2 \text{ gN}^{-1}$
Fraction oxygen in water at sediment-water interface	fo	0.6	-
Fraction reduced substances retained from oxidation;			
mean	fro	0.0	-
amplitude		0.0	-
period		365	d
phase		0.2	-

¹⁾ The incorp. rate is dealt with in the input for S1 detritus as a burial rate in 1/d, that can be made approx. temperature dependent by providing a time dependent function.

²⁾ The decomposition rates and temperature coefficients for detritus in the boundary layer are input for the S1 module of DELWAQ. Rates and coefficients have to be provided for org. C, org. N and org. P.

3 Aerobic layer and the sediment oxygen demand

The thickness of the aerobic layer is dependent on the oxygen consumption rate according to the following steady-state equation:

$$d_1 = \sqrt{2 \cdot p_1 \cdot D \cdot f_o \cdot C_{O_0} / R_o} \quad (3.1)$$

$$d_1 = d_{1m} \quad \text{if } d_1 < d_{1m}$$

in which:

C_{O_0}	oxygen concentration in the overlying water [g m^{-3}]
d_{1m}	minimal thickness of the aerobic layer [m]
D	dispersion coefficient [$\text{m}^2 \text{d}^{-1}$]
f_o	ratio of the oxygen concentrations at the upper and lower sides of the water boundary layer [-]
p	porosity [-]
R_o	oxygen consumption rate [$\text{g m}^3 \text{bottom d}^{-1}$]

A subscript figure indicates a layer number or an interface number!

The introduction of ratio f_o relates to the existence of a relatively stagnant boundary layer in the overlying water, which contains a part of the oxygen gradient at the sediment-water interface. The oxygen concentration at the interface is a certain fraction of the average oxygen concentration in the water column.

Oxygen is consumed in the degradation of detritus in the boundary layer (complex-detritus in the terminology of DBS) and of detritus in the aerobic layer, in the nitrification and in the chemical oxidation. The oxygen consumption rate R_o is formulated as follows:

$$R_o = F_{o_b} / d_1 + a_c \cdot k_{c_1} \cdot C_{d_1} + p_1 \cdot a_n \cdot k_n \cdot C_{a_1} + F_{o_c} / d_1 \quad (3.2)$$

in which:

a_c	stoichiometric constant [$\text{gO}_2 \text{gC}^{-1}$]
a_n	stoichiometric constant [$\text{gO}_2 \text{gN}^{-1}$]
C_{d_1}	detritus concentration in the upper layer [$\text{gC m}^{-3} \text{B}$]
C_{a_1}	ammonium concentration in the aerobic layer [$\text{gN m}^{-3} \text{PW}$]
F_{o_b}	oxygen consumption in the boundary layer [$\text{gO}_2 \text{m}^{-2} \text{d}^{-1}$]
F_{o_c}	chemical oxygen demand [$\text{gO}_2 \text{m}^{-2} \text{d}^{-1}$]
k_{c_1}	degradation rate of detritus in the upper layer [d^{-1}]
k_n	nitrification rate [d^{-1}], equal to zero if $C_{O_0} = 0.0$

The oxygen consumption in the boundary layer is connected with the degradation of detritus on top of the sediments and is equal to:

$$F_{o_b} = a_c \cdot k_{c_b} \cdot C_{d_b} \quad (3.3)$$

in which:

C_{d_b}	amount of complex-detritus in the boundary layer [gC m^2]
k_{c_b}	degradation rate of complex-detritus in the boundary layer [d^{-1}]

The chemical oxygen demand concerns the oxidation of reduced substances, such as iron(II), manganese(II), sulphide and methane originating from the degradation of detritus in the anaerobic part of the 'active' bottom. However, the reduced substances will not be oxidising completely. A part of the sulphide resulting from sulphate reduction precipitates with iron and may



accumulate in the reduced part of the sediments. Methane may escape from the sediments in gas bubbles. Consequently, the actual chemical oxygen demand is formulated as a fraction of the potential chemical oxygen demand:

$$Fo_c = (1 - fro) \cdot ac \cdot (kc_1 \cdot Cd_1 \cdot (d_2 + d_3) + kc_4 \cdot Cd_4 \cdot d_4) \quad (3.4)$$

in which:

fro fraction reduced substances permanently removed or fixed [-]
kc₄ degradation rate of detritus in the lower layer [d⁻¹]

Note that the degradation of detritus in the denitrifying layer has been included entirely in the chemical oxygen demand. This is not correct as such, since the elementary nitrogen produced by denitrification is chemically inert. It is not oxidised, but escapes from the bottom. A correction for the amount of nitrate consumed by denitrification can be made with fro. No correction was made in the second version of SWITCH.

The sediment oxygen demand is quantified with:

$$Fo = Fo_b + (ac \cdot kc_1 \cdot Cd_1 + p_1 \cdot an \cdot kn \cdot Ca_1) \cdot d_1 + Fo_c \quad (3.5)$$

Maintaining a bottom oxygen demand under anaerobic conditions in the water column (kn = 0.0!) leads to a negative oxygen concentration in the water quality model representing the surplus of reduced substances.

4 Denitrifying layer and nitrate

Nitrate is formed from ammonium through nitrification in the aerobic top layer. It is subjected to vertical transport and denitrification in the zone just below this layer (Vanderborght *et al.*, 1977a). The thickness of the denitrifying layer follows from the (approximate) steady-state solution of the differential equation for nitrate in this layer:

$$\begin{aligned} d_2 &= 2(Cn_1 - Cn_c)/Cn_1 \cdot \sqrt{D/kd} \\ d_2 &= 0.0 \quad \text{if } Cn_1 \leq Cn_c \end{aligned} \quad (4.1)$$

in which:

kd	first order denitrification rate [d^{-1}]
Cn_1	nitrate concentration in the top layer [$gN\ m^{-3}$]
Cn_c	critical nitrate concentration [$gN\ m^{-3}$]

The critical nitrate concentration is the maximal concentration at which sulphate reduction is possible, about $0.1\ gN\ m^{-3}$.

The nitrate concentration in the aerobic and denitrifying layers follow from:

$$\frac{dCn_1}{dt} = (Fn_b - Fn_0 + Fn_1)/(p_1 \cdot d_1) + kn \cdot Ca_1 \quad (4.2)$$

with:

$$\begin{aligned} Fn_0 &= 2p_1 \cdot D \cdot (Cn_1 - Cn_0)/(l + d_1) \\ Fn_1 &= -2p_1 \cdot kd \cdot Cn_2 \cdot \sqrt{D/kd} \\ Cn_2 &= \frac{1}{2}Cn_1 \end{aligned}$$

in which:

Ca_1	ammonium concentration in the top layer [$gN\ m^{-3}$]
Fn_b	flux from the boundary layer [$gN\ m^{-2}\ d^{-1}$]
Fn_0	dispersive return flux to the overlying water [$gN\ m^{-2}\ d^{-1}$]
Fn_1	flux to the denitrifying layer [$gN\ m^{-2}\ d^{-1}$]
l	thickness of the water boundary layer [m]



DRAFT

5 Detritus

Organic carbon

All organic matter, which settles on the sediments is considered as detritus, regardless of its origin. GEM distinguishes:

- ◇ live phytoplankton, which enters the complex-detritus pool in the boundary layer due to settling;
- ◇ dead microphytobenthos, which enters the complex-detritus pool in the boundary layer due to mortality;
- ◇ fast decomposing detritus and slow decomposing detritus, that enter the complex-detritus pool in the boundary layer as the net result of settling and resuspension; and
- ◇ refractory detritus, which enters the slow decomposing detritus pool in the lower layer due to settling.

SWITCH transfers the complex-detritus to the relatively fast decomposing sediment-detritus pool. Resuspension (if occurring) leads to reincorporation of the detritus into the water column as fast decomposing detritus. The model converts a fraction of the sediment-detritus into refractory humic matter, which is stored in the sediment.

Summarising, detritus is subjected to settling, resuspension, incorporation from the boundary layer into the sediment, degradation, humification and burial (Bernier, 1974). The degradation rate decreases while the organic matter is transported downwards in the sediment.

The concentrations of detritus in the boundary layer and the bottom layers are described with the following differential equations:

$$\frac{dCd_b}{dt} = Fd_s - Fd_b - kc_b \cdot Cd_b \quad (5.1)$$

$$\frac{dCd_1}{dt} = (Fd_b - Fb_3 \cdot Cd_1 + Fd_3)/dh - kc_1 \cdot Cd_1 \quad (5.2)$$

$$\frac{dCd_4}{dt} = (Fxd_s + Fb_3 \cdot Cd_1 - Fd_3)/d_4 - (1 + frf) \cdot kc_4 \cdot Cd_4 \quad (5.3)$$

with:

$$Fd_s = sc \cdot Cd_0$$

$$Fd_b = rc \cdot Cd_b$$

$$Fb_3 = Fs - Fr \geq 0.0$$

$$Fb_4 = Fb_3 \cdot (1 - p_1)/(1 - p_4)$$

$$Fd_3 = 2Db \cdot (Cd_4/(1 - p_4) - Cd_1/(1 - p_1))/(dh + d_4)$$

$$Fxd_s = sc \cdot Cxd_0$$

in which:

Cd_0 detritus concentration in the overlying water [$gC m^{-3}$]

Cd_b amount of detritus in the boundary layer [$gC m^{-2}$]

Cd_1 detritus concentration in the upper layer [$gC m^{-3}B$]

Cd_4 detritus concentration in the lower layer [$gC m^{-3}B$]

Cxd_0 refractory detritus concentration in the overlying water [$g m^{-3}$]

Db bioturbation dispersion coefficient ($m^2 d^{-1}$)

frf factor for the conversion of detritus into refractory organic matter [-]

Fb burial flux based on displaced bottom volume ($m^3B m^{-2} d^{-1}$)



Fd	bioturbation flux [gC m ⁻² d ⁻¹]
Fd _b	flux of detritus incorporated in the upper layer [gC m ⁻² d ⁻¹]
Fd _s	flux of detritus settled from the overlying water [gC m ⁻² d ⁻¹]
Fr	resuspension flux based on displaced bottom volume [m ³ B m ⁻² d ⁻¹]
Fs	sedimentation flux based on displaced bottom volume [m ³ B m ⁻² d ⁻¹]
kc _b	degradation rate of detritus in the boundary layer [d ⁻¹]
rc	rate of incorporation in the upper layer [d ⁻¹]
sc	sedimentation rate for detritus [m d ⁻¹]
Fxd _s	flux of refractory detritus incorporated in the sediment [gC m ⁻² d ⁻¹]

The amount of detritus in the boundary layer (Cd_b) is not calculated in SWITCH itself but in the S1 sediment module of DELWAQ (DBS or GEM). The decomposition rate and the incorporation (burial) rate are input to this S1 module.

Notice that the conversion of detritus into refractory organic matter has been formulated as a process that is proportional and additive to decomposition at the same time. frf can be seen as an amplification factor. frf/(1 - frf) delivers the fraction of the degradable organic matter that is converted into refractory organic matter.

SWITCH has input parameters with respect to settling and resuspension. The difference Fs - Fr is in fact the net sediment accretion rate or the burial rate in case of a positive value, not to be confused with the incorporation rate, which may also be called a burial rate. Notice that the formulations in SWITCH regarding detritus are only valid for burial. Moreover, it is assumed that all detritus has been degraded or converted before it arrives at the lower boundary of the 'active' bottom layer, so that burial does not remove degradable detritus from the lower layer.

Only the 'average' concentration of the refractory organic matter is calculated for the 'active' bottom. The concentration is derived from:

$$\frac{dCrd_1}{dt} = (-Fb_4 \cdot Crd_1 + frf \cdot kc_4 \cdot Cd_4 \cdot d_4) / (dh + d_4) \quad (5.4)$$

Organic nitrogen

Similar equations have been formulated for organic nitrogen. The decomposable organic nitrogen in detritus is converted into ammonium and into refractory organic nitrogen in the following way:

$$\frac{dCnd_b}{dt} = Fnd_s - Fnd_b - knd_b \cdot Cnd_b \quad (5.5)$$

$$\frac{dCnd_1}{dt} = (Fnd_b - Fb_3 \cdot Cnd_1 + Fnd_3) / dh - (1 + fa_1) \cdot kc_1 \cdot Cnd_1 \quad (5.6)$$

$$\frac{dCnd_4}{dt} = (Fxn_s + Fb_3 \cdot Cnd_1 - Fnd_3) / d_4 - (1 + fa_4 + frf) \cdot kc_4 \cdot Cnd_4 \quad (5.7)$$

with:

$$fa_1 = (Cnd_1 / Cd_1 - aa) / aa$$

$$fa_4 = (Cnd_4 / Cd_4 - aa) / aa$$

$$Fnd_s = sc \cdot Cnd_0$$

$$Fnd_b = rc \cdot Cnd_b$$

$$Fnd_3 = 2Db \cdot (Cnd_4 / (1 - p_4) - Cnd_1 / (1 - p_1)) / (dh + d_4)$$

$$Fxn_s = sc \cdot Cxn_0$$

in which:

aa	stoichiometric constant for nitrogen in refractory detritus [gN gC ⁻¹]
Cnd ₀	detritus nitrogen concentration in the overlying water [gN m ⁻³]
Cnd _b	amount of detritus nitrogen in the boundary layer [gN m ⁻²]
Cnd ₁	detritus nitrogen concentration in the upper layer [gN m ⁻³ B]
Cnd ₄	detritus nitrogen concentration in the lower layer [gN m ⁻³ B]
Cxn ₀	slow decomposing detritus nitrogen (OON) concentration in overlying water [gN m ⁻³]
fa	correction factor for organic nitrogen degradation rate [-]
Fnd	bioturbation flux [gN m ⁻² d ⁻¹]
Fnd _b	flux of detritus nitrogen incorporated in the upper layer [gN m ⁻² d ⁻¹]
Fnd _s	flux of detritus nitrogen settled from the overlying water [gN m ⁻² d ⁻¹]
Fxn _s	flux of slow decomposing detritus nitrogen (OON) incorp. in sediment [gN m ⁻² d ⁻¹]
knd _b	degradation rate of detritus nitrogen in the boundary layer [d ⁻¹]

The amount of detritus nitrogen in the boundary layer (Cnd_b) is not calculated in SWITCH itself but in the S1 sediment module of DELWAQ (DBS or GEM). The decomposition rate and the incorporation (burial) rate are input to this S1 module.

The degradation rates of organic nitrogen are adjusted in such a way that the organic matter is gradually stripped from nitrogen in excess of the nitrogen in refractory organic matter.

The 'sediment-average' concentration of the refractory organic nitrogen follows from:

$$\frac{dCrn_1}{dt} = (-Fb_4 \cdot Crn_1 + frf \cdot kc_4 \cdot Cnd_4 \cdot d_4)/(dh + d_4) \quad (5.8)$$

Organic phosphorus

The following equations describe the organic phosphorus in accordance with the above:

$$\frac{dCpd_b}{dt} = Fpd_s - Fpd_b - kpd_b \cdot Cpd_b \quad (5.9)$$

$$\frac{dCpd_1}{dt} = (Fpd_b - Fb_3 \cdot Cpd_1 + Fnd_3)/dh - (1 + fp_1) \cdot kc_1 \cdot Cpd_1 \quad (5.10)$$

$$\frac{dCpd_4}{dt} = (Fxp_s + Fb_3 \cdot Cpd_1 - Fnd_3)/d_4 - (1 + fp_4 + frf) \cdot kc_4 \cdot Cpd_4 \quad (5.11)$$

with:

$$fp_1 = (Cpd_1/Cd_1 - ap)/ap$$

$$fp_4 = (Cpd_4/Cd_4 - ap)/ap$$

$$Fpd_s = sc \cdot Cpd_0$$

$$Fpd_b = rc \cdot Cpd_b$$

$$Fpd_3 = 2Db \cdot (Cpd_4/(1 - p_4) - Cpd_1/(1 - p_1))/(dh + d_4)$$

$$Fxp_s = sc \cdot Cxp_0$$

in which:

ap	stoichiometric constant for phosphorus in refractory detritus [gP gC ⁻¹]
Cpd ₀	detritus phosphorus concentration in the overlying water [gP m ⁻³]
Cpd _b	amount of detritus phosphorus in the boundary layer [gP m ⁻²]
Cpd ₁	detritus phosphorus concentration in the upper layer [gP m ⁻³ B]
Cpd ₄	detritus phosphorus concentration in the lower layer [gP m ⁻³ B]

C_{xp_0}	slow decomposing detritus phosphorus (OOP) concentration overlying water [gP m ⁻³]
f_p	correction factor for organic phosphorus degradation rate [-]
F_{pd}	bioturbation flux [gP m ⁻² d ⁻¹]
F_{pd_b}	flux of detritus phosphorus incorporated in the upper layer [gP m ⁻² d ⁻¹]
F_{pd_s}	flux of detritus phosphorus settled from the overlying water [gP m ⁻² d ⁻¹]
F_{xp_s}	flux of slow decomp. detritus phosphorus (OOP) incorp. in sediment [gP m ⁻² d ⁻¹]
k_{pd_b}	degradation rate of detritus phosphorus in the boundary layer [d ⁻¹]

The amount of detritus phosphorus in the boundary layer (C_{nd_b}) is not calculated in SWITCH itself but in the S1 sediment module of DELWAQ (DBS or GEM). The decomposition rate and the incorporation (burial) rate are input to this S1 module.

The 'sediment-average' concentration of the refractory organic phosphorus follows from:

$$\frac{dC_{rp_1}}{dt} = (-F_{b_4} \cdot C_{rp_1} + f_{rf} \cdot k_{c_4} \cdot C_{pd_4} \cdot d_4) / (d_h + d_4)$$

6 Ammonium

Ammonium is released the degradation of detritus and is nitrified by bacteria under aerobic conditions (Berner, 1974; Vanderborght *et al.*, 1977b). Ammonium adsorbs to a certain extent to clays in the sediments. The adsorption equilibrium is pH dependent. It is estimated that about 25 to 50 % of the ammonium present in silty sediments may be adsorbed (partition coefficient ≈ 1). This is a relatively small quantity compared to the high turn-over rates of ammonium in sediments. Thus, the adsorption offers only a small buffering capacity, which implies that no large mass fluxes are involved in the adsorption of ammonium. A change of ammonification is quickly followed by a proportional change of the ammonium concentration in the pore water. It is therefore justified to ignore the adsorption of ammonium in SWITCH.

The ammonium concentrations in the aerobic top layer, the remaining part of the upper layer (d_2+d_3) and the lower reducing layer (d_l) are described with:

$$\frac{dCa_1}{dt} = (Fa_b - Fa_0 + Fa_1 + Fas_0 - Fas_1)/(p_1 \cdot d_1) + (1 + fa_1) \cdot kc_1 \cdot Cnd_1/p_1 - kn \cdot Ca_1 \quad (6.1)$$

$$\frac{dCa_2}{dt} = (-Fa_1 + Fa_3 + Fas_1 - Fas_3)/(p_1 \cdot (d_2 + d_3)) + (1 + fa_1) \cdot kc_1 \cdot Cnd_1/p_1 \quad (6.2)$$

$$\frac{dCa_4}{dt} = (-Fa_3 + Fas_3 - Fas_4)/(p_4 \cdot d_4) + (1 + fa_4) \cdot kc_4 \cdot Cnd_4/p_4 \quad (6.3)$$

with:

$$Fa_b = knd_b \cdot Cd_b$$

$$Fa_0 = 2p_1 \cdot D \cdot (Ca_1 - Ca_0)/(l + d_1)$$

$$Fa_1 = 2p_1 \cdot D \cdot (Ca_2 - Ca_1)/d_0$$

$$Fa_3 = (p_1 + p_4) \cdot D \cdot (Ca_4 - Ca_2)/(d - d_1)$$

$$Fas_0 = -vs \cdot Ca_0 \quad \text{if } vs < 0.0$$

$$Fas_1 = -vs \cdot Ca_1$$

$$Fas_3 = -vs \cdot Ca_2$$

$$Fas_4 = -vs \cdot Ca_4$$

$$Fas_0 = -vs \cdot Ca_1 \quad \text{if } vs > 0.0$$

$$Fas_1 = -vs \cdot Ca_2$$

$$Fas_3 = -vs \cdot Ca_4$$

$$Fas_4 = -vs \cdot Ca_5$$

in which:

Ca_5	ammonium concentration in the lower boundary layer [$gN m^{-3}$]
Fa_b	flux from degradation detritus in boundary layer [$gN m^{-2} d^{-1}$]
Fa_0	dispersive return flux to the overlying water [$gN m^{-2} d^{-1}$]
Fa_{1-3}	dispersive flux between two adjacent layers [$gN m^{-2} d^{-1}$]
Fas_0	seepage flux at the sediment-water interface [$gN m^{-2} d^{-1}$]
Fas_{1-3}	seepage flux between two adjacent layers [$gN m^{-2} d^{-1}$]



F_{as_4}	seepage flux at the lower boundary [$\text{gN m}^{-2} \text{d}^{-1}$]
knd_b	degradation rate of detritus nitrogen in the boundary layer [d^{-1}]
vs	seepage velocity [m d^{-1}]

It is assumed that no dispersive transport occurs across the interface of the 'active' and 'inactive' parts of the bottom. The assumption implies that the concentration of a dissolved substance is the same at both sides of the lower boundary of the bottom in the model. It is a reasonable assumption when seasonal variations in the concentration of a dissolved substance is small at the lower boundary. Moreover, a long-term shift in the ammonium concentration in the 'inactive' bottom does hardly affect the sediment-water exchange fluxes.

SWITCH stops nitrification ($kn = 0.0$) when the dissolved oxygen concentration in the water column is equal to or less than 0.0.

7 Phosphate

Bacterial activity liberates phosphate from organic matter just like ammonium. In contrast with ammonium, phosphate adsorbs strongly to several components of the sediments, the hydroxides of iron(III) and aluminum in particular. Iron(III) hydroxide is present in a relatively high concentration in the oxidising layer, where it is stable. The concentration declines at the interface of the oxidising and reducing layers and goes down further in the reducing layer under the influence of reduction processes. Consequently, the adsorption is much stronger in the oxidising layer than in the reducing layer (Van Raaphorst *et al.* (1988); Brinkman and Van Raaphorst (1986); Lijklema (1980); Berner (1974)).

Phosphate also precipitates in minerals, the identity of which has not been determined unequivocally (WL | Delft Hydraulics, 1994a). Vivianite (iron(II)phosphate) is being mentioned as the main mineral, but vivianite is not stable under oxidising conditions. Apatite (calcium phosphate) may be present as a stable mineral in marine water sediments. Coprecipitation with several carbonates and sulphides is also possible.

SWITCH assumes equilibrium for the adsorption process, whereas precipitation and dissolution are formulated as slow processes. The assumption of equilibrium has the advantage, that only inorganic phosphate and precipitated phosphate need to be calculated explicitly on the basis of mass balances. The dissolved and adsorbed phosphate concentrations follow from the equilibrium condition for adsorption. The following four fractions are distinguished:

$$\begin{aligned}C_{pp} &= f_{pp} \cdot C_p \\C_{mp} &= f_{mp} \cdot C_p \\C_{dp} &= f_{dp} \cdot C_p/p \\C_{ap} &= f_{ap} \cdot C_p\end{aligned}\tag{7.1}$$

$$f_{ap} + f_{dp} + f_{pp} + f_{mp} = 1$$

in which:

C_p	total inorganic phosphate concentration [gP m ⁻³ B]
C_{ap}	adsorbed phosphate concentration [gP m ⁻³ B]
C_{dp}	dissolved phosphate concentration [gP m ⁻³ PW]
C_{mp}	concentration of phosphate in a stable mineral [gP m ⁻³ B]
C_{pp}	concentration of phosphate in vivianite [gP m ⁻³ B]
f_{ap}	adsorbed fraction [-]
f_{dp}	dissolved fraction [-]
f_{mp}	stable mineral fraction [-]
f_{pp}	vivianite fraction [-]

These fractions are relevant for the mass balance equation for total inorganic phosphate, because the processes affect only one or two of the fractions.

The mineral phosphate fractions can be determined after solution of the mass balance equations for these components. The precipitation process is formulated with first order kinetics. The driving force is the difference between the actual concentration and the saturation concentration of ortho-phosphate dissolved in the pore water. In principle, the latter may be determined from the solubility product of the phosphate mineral, when its identity has been established. No distinction was made between the precipitation rates and the saturation concentrations of vivianite and the stable mineral, as the in-situ properties of these minerals are unknown. The precipitation rate is a function of the driving force, the nature of which depends



on the rate limiting mechanism. The function is linear when diffusion to the surface of the mineral is the rate limiting process. In case that the surface reaction is rate limiting, the function may be non-linear. However, the assumption of simple first order reaction kinetics ignoring the role of coprecipitants seems reasonable in this stage, considering that the precipitation rate has not yet been determined accurately and that the dissolved iron concentration is not simulated.

The development of the concentrations of the stable mineral phosphate is described with:

$$\begin{aligned} \frac{d C_{mp_1}}{dt} = & p_1 \cdot f_m \cdot k_p \cdot (f_{dp_1} \cdot C_{p_1}/p_1 - C_{dp_s}) + \\ & (-Fr \cdot f_{mp_1} \cdot C_{p_1} - Fb_2 \cdot f_{mp_1} \cdot C_{p_1})/d_o + \\ & 2Db \cdot (f_{mp_3} \cdot C_{p_3} - f_{mp_1} \cdot C_{p_1})/(1 - p_1)/(d_o + d_3)/d_o \end{aligned} \quad (7.2)$$

$$\begin{aligned} \frac{d C_{mp_3}}{dt} = & p_1 \cdot f_m \cdot k_p \cdot (f_{dp_3} \cdot C_{p_3}/p_1 - C_{dp_s}) + \\ & (Fb_2 \cdot f_{mp_1} \cdot C_{p_1} - Fb_3 \cdot f_{mp_3} \cdot C_{p_3})/d_3 - \\ & 2Db \cdot (f_{mp_3} \cdot C_{p_3} - f_{mp_1} \cdot C_{p_1})/(1 - p_1)/(d_o + d_3)/d_3 + \\ & 2Db \cdot (f_{mp_4} \cdot C_{p_4}/(1 - p_4) - f_{mp_3} \cdot C_{p_3}/(1 - p_1))/(d_3 + d_4)/d_3 \end{aligned} \quad (7.3)$$

$$\begin{aligned} \frac{d C_{mp_4}}{dt} = & p_4 \cdot f_m \cdot k_p \cdot (f_{dp_4} \cdot C_{p_4}/p_4 - C_{dp_s}) + \\ & (Fb_3 \cdot f_{mp_3} \cdot C_{p_3} - Fb_4 \cdot f_{mp_4} \cdot C_{p_4})/d_4 - \\ & 2Db \cdot (f_{mp_4} \cdot C_{p_4}/(1 - p_4) - f_{mp_3} \cdot C_{p_3}/(1 - p_1))/(d_3 + d_4)/d_4 \end{aligned} \quad (7.4)$$

in which:

C_{dp_s}	saturation concentration for dissolved ortho-phosphate [$gP \text{ m}^{-3}PW$]
f_m	fraction of precipitated phosphorus stored in the stable mineral [-]
Fr	resuspension flux based on bottom volume [$m^3 \text{ m}^{-2} \text{ d}^{-1}$]
k_p	precipitation rate [d^{-1}]

Vivianite forms in the reducing parts of the sediments. It dissolves gradually when transported into the oxidising layer by means of bioturbation of the sediments. This hypothesis can be justified as follows:

- ◇ Vivianite (iron(II) phosphate) is unstable under oxidising conditions (Lijklema, 1980).
- ◇ The concentration of dissolved Fe(II), and in some parts also the concentration of dissolved ortho-phosphate, is much higher in the reducing layer than in the oxidising layer. The solubility product is probably only exceeded in the reducing layer.

The formulation of the dissolution process is not straight forward. The dissolution is probably characterised by two steps: a) the oxidation of dissolved Fe^{2+} , b) the dissolution of vivianite at a very low dissolved Fe^{2+} -concentration. The driving force may therefore be the difference between the Fe^{2+} -concentration near the vivianite crystals and the average dissolved Fe^{2+} -concentration. The latter may approximately be equal to zero, due to oxidation.

The dissolution rate may then be formulated as follows:

$$R_{dis} = k_{dis} \cdot C_{pp} \cdot C_{fe} \quad (7.5)$$

in which:

C_{fe}	dissolved Fe^{2+} -concentration near the surface of vivianite crystals [$gFe \text{ m}^{-3}$]
k_{dis}	(second order) dissolution rate constant [$m^3 \text{ gFe}^{-1} \text{ d}^{-1}$]

R_{dis} dissolution rate [$gP\ m^{-3}\ d^{-1}$]

The dissolved Fe^{2+} -concentration near the surface of the crystals is calculated from the solubility product (equilibrium constant) and the dissolved phosphate concentration with:

$$C_{fe} = (L_s / C_{dp}^2)^{0.33} \quad (7.6)$$

in which:

L_s solubility product of vivianite

Equations 7.5–7.6 have been combined to make the dissolution rate dependent on the dissolved phosphate concentration (power -0.67). The solubility product becomes an implicit part of the dissolution rate constant. The resulting formulation meets the demand that the dissolution process slows down when the dissolved phosphate concentration increases.

The mass balances for phosphate in vivianite in three layers are:

$$\begin{aligned} \frac{dC_{pp1}}{dt} = & -kdp \cdot f_{pp1} \cdot C_{p1} \cdot (fdp_1 \cdot C_{p1} / p_1)^{-0.67} + \\ & (-Fr \cdot f_{pp1} \cdot C_{p1} - Fb_2 \cdot f_{pp1} \cdot C_{p1}) / do + \\ & 2Db \cdot (f_{pp3} \cdot C_{p3} - f_{pp1} \cdot C_{p1}) / (1 - p_1) / (do + d_3) / do \end{aligned} \quad (7.7)$$

$$\begin{aligned} \frac{dC_{pp3}}{dt} = & p_1 \cdot kp \cdot (fdp_3 \cdot C_{p3} / p_1 - C_{dp_s}) + \\ & (Fb_2 \cdot f_{pp1} \cdot C_{p1} - Fb_3 \cdot f_{pp3} \cdot C_{p3}) / d_3 - \\ & 2Db \cdot (f_{pp3} \cdot C_{p3} - f_{pp1} \cdot C_{p1}) / (1 - p_1) / (do + d_3) / d_3 + \\ & 2Db \cdot (f_{pp4} \cdot C_{p4} / (1 - p_4) - f_{pp3} \cdot C_{p3} / (1 - p_1)) / (d_3 + d_4) / d_3 \end{aligned} \quad (7.8)$$

$$\begin{aligned} \frac{dC_{pp4}}{dt} = & p_4 \cdot kp \cdot (fdp_4 \cdot C_{p4} / p_4 - C_{dp_s}) + \\ & (Fb_3 \cdot f_{pp3} \cdot C_{p3} - Fb_4 \cdot f_{pp4} \cdot C_{p4}) / d_4 - \\ & 2Db \cdot (f_{pp4} \cdot C_{p4} / (1 - p_4) - f_{pp3} \cdot C_{p3} / (1 - p_1)) / (d_3 + d_4) / d_4 \end{aligned} \quad (7.9)$$

in which:

kdp dissolution rate ($m^{-2.01}\ gP^{0.67}\ d^{-1}$)

The dissolved fraction can be derived from the following Langmuir adsorption isotherm:

$$C_{ap} = C_{am} \cdot C_{dp} / (K_s + C_{dp}) \quad (7.10)$$

$$C_{am} = C_{ac} \cdot (1 - p) \cdot W_s$$

in which:

C_{ac} adsorption capacity [$gP\ kg^{-1}DM$]

C_{am} maximal concentration of adsorbed phosphate [$gP\ m^{-3}B$]

K_s half saturation concentration [$gP\ m^{-3}PW$]

W_s specific weight of the sediments [$kg\ m^{-3}$]

The adsorption capacity depends on the oxidising iron (III) and aluminum contents of the sediments. This sediment property is different for the oxidising layer and the reducing layer. The oxidising iron content and (therefore) the adsorption capacity decrease in a downward direction. Iron(III) is reduced to iron(II) in connection with the degradation of organic matter. The oxidising iron gradient is smoothed by bioturbation of the sediment, which results in upward transport of iron(II) formed in the reducing layer and in downward transport of iron(III) formed

in the oxidising layer. Moreover, the adsorption capacities change in time due to changes of the temperature dependent rates of degradation of organic matter and bioturbation. Both processes affect the position of the interface between the layers and the amounts of oxidising iron present in the layers. This is taken into account in SWITCH, whereas the dependency on pH and salinity of the adsorption parameters is not considered explicitly.

Tentative simulations with the complex chemical model HADES showed that the iron(III) contents of the oxidising layer and the reducing layer are related to the thickness of the oxidising layer (WL | Delft Hydraulics, 1991). The adsorption capacity increases with increasing thickness of the oxidising layer. However, it has not been possible yet to formulate this relation deterministically. Empirical relations, determined by means of model calibration for Lake Veluwe, have been introduced in SWITCH in stead. The relations used in SWITCH are:

$$\begin{aligned} \text{Cam}_1 &= \text{fac}_1 \cdot \text{Cac} \cdot (1 - p_1) \cdot W_s \\ \text{Cam}_3 &= \text{fac}_1 \cdot \text{fac}_3 \cdot \text{Cac} \cdot (1 - p_1) \cdot W_s \\ \text{Cam}_4 &= 0.5 \text{fac}_4 \cdot \text{Cac} \cdot (1 - p_4) \cdot W_s \\ \text{fac}_1 &= ((d_1 + d_2)/0.005)^{0.25} \\ \text{fac}_3 &= ((d_1 + d_2)/dh)^{0.25} \\ \text{fac}_4 &= dh/(dh + d_4) \end{aligned}$$

in which:

Cam_1	maximal concentration of adsorbed phosphate in the oxidising layer [gP m ⁻³ B]
Cam_3	maximal concentration of adsorbed phosphate in the upper reducing layer [gP m ⁻³ B]
Cam_4	maximal concentration of adsorbed phosphate in the lower reducing layer [gP m ⁻³ B]
Cac	time average adsorption capacity of the oxidising layer [gP kg ⁻¹ DM]
fac	empirical factor linking up the ads. capacity with layer thickness [-]

The adsorption capacity of the oxidising layer becomes bigger than the 'average' capacity (Cac) when the thickness of the oxidising layer becomes bigger than 0.005 m, which is about half the maximal thickness of the oxidising layer. The adsorption capacities of the reducing layers depend also on the values of dh and d4 (input parameters for SWITCH). The thicker the reducing layers are, the smaller their depth average adsorption capacities are. This is logical considering the fact that the capacity decreases with depth.

The adsorption capacity of the oxidising layer is set equal to the capacity of the upper reducing layer, when the depth of the oxidising layer ($d_o=d_1+d_2$) becomes smaller than critical thickness d_{om} . It is assumed in fact that the excess adsorption capacity in the upper layer disappears completely, when the oxidising layer collapses. Consequently, the concentration gradient of dissolved phosphate increases steeply, which generates so-called "explosive" phosphate return fluxes.

An earlier approach, which defined the adsorption capacities of the lower reducing layer 4 as a constant fraction (=0.2) of the adsorption capacity of the upper reducing layer 3, is also available in SWITCH as an alternative option.

SWITCH requires input for the adsorption capacity of the oxidising top layer (layers 1–2) and the adsorption capacity of the upper reducing layer 3. The model uses the constant ratio option when the adsorption capacity of the upper reducing layer is given a positive value. In case this parameter obtains a negative value (for instance -999), the layer depth dependent option is applied.

A quadratic equation in fdp is obtained when equation 7.10 is substituted in equations 7.1. The positive root is:

$$fdp = \left\{ (1 - fmp - fpp) \cdot Cp - p \cdot Ks - Cam + \sqrt{\left((1 - fmp - fpp) \cdot Cp - p \cdot Ks - Cam \right)^2 + 4(1 - fmp - fpp) \cdot Cp \cdot p \cdot Ks} \right\} / (2Cp) \quad (7.11)$$

Having defined all four phosphate fractions, the mass balances for total inorganic phosphate in the oxidising layer, the upper reducing layer and the lower reducing layer have been formulated as follows:

$$\frac{dCp_1}{dt} = (Fp_b + Fp_s - Fp_0 + Fp_2 + Fps_0 - Fps_2 - Fr \cdot Cp_1 + Fpd_2 - Fb_2 \cdot Cp_1) / do + (1 + fp_1) \cdot kc_1 \cdot Cpd_1 \quad (7.12)$$

$$\frac{dCp_3}{dt} = (-Fp_2 + Fp_3 + Fps_2 - Fps_3 - Fpd_2 + Fpd_3 + Fb_2 \cdot Cp_1 - Fb_3 \cdot Cp_3) / d_3 + (1 + fp_1) \cdot kc_1 \cdot Cpd_1 \quad (7.13)$$

$$\frac{dCp_4}{dt} = (-Fp_3 + Fps_3 - Fps_4 - Fpd_3 + Fb_3 \cdot Cp_3 - Fb_4 \cdot Cp_4) / d_4 + (1 + fp_4) \cdot kc_4 \cdot Cpd_4 \quad (7.14)$$

with:

$$Fp_b = kpd_b \cdot Cpd_b$$

$$Fp_0 = 2p_1 \cdot D \cdot (fdp_1 \cdot Cp_1 / p_1 - fdp_0 \cdot Cp_0) / (l + do)$$

$$Fp_2 = 2D \cdot (fdp_3 \cdot Cp_3 - fdp_1 \cdot Cp_1) / (do + d_3)$$

$$Fp_3 = (p_1 + p_4) \cdot D \cdot (fdp_4 \cdot Cp_4 / p_4 - fdp_3 \cdot Cp_3 / p_1) / (d_3 + d_4)$$

$$Fpd_2 = 2Db \cdot ((fpp_3 + fmp_3 + fap_3) \cdot Cp_3 - (fmp_1 + fap_1) \cdot Cp_1) / (1 - p_1) / (do + d_3)$$

$$Fpd_3 = 2Db \cdot ((fpp_4 + fmp_4 + fap_4) \cdot Cp_4 / (1 - p_4) - (fpp_3 + fmp_3 + fap_3) \cdot Cp_3 / (1 - p_1)) / (d_3 + d_4)$$

$$Fps_0 = -vs \cdot fdp_0 \cdot Cp_0 / p_1 \quad \text{if } vs < 0 \cdot 0$$

$$Fps_2 = -vs \cdot fdp_1 \cdot Cp_1 / p_1$$

$$Fps_3 = -vs \cdot fdp_3 \cdot Cp_3 / p_1$$

$$Fps_4 = -vs \cdot fdp_4 \cdot Cp_4 / p_4$$

$$Fps_0 = -vs \cdot fdp_1 \cdot Cp_1 / p_1 \quad \text{if } vs > 0 \cdot 0$$

$$Fps_2 = -vs \cdot fdp_3 \cdot Cp_3 / p_1$$

$$Fps_3 = -vs \cdot fdp_4 \cdot Cp_4 / p_4$$

$$Fps_4 = -vs \cdot Cdp_5$$

in which:

Cdp_5 dissolved phosphate concentration in the lower boundary layer [$gP \cdot m^{-3}$]

Fb burial flux based on sediment volume [$m^3 \cdot m^{-2} \cdot d^{-1}$]

Fr resuspension flux based on sediment volume [$m^3 \cdot m^{-2} \cdot d^{-1}$]

Fp_b flux from degradation detritus in boundary layer [$gP \cdot m^{-2} \cdot d^{-1}$]

F_{p_s}	sedimentation flux of adsorbed phosphate [$\text{gP m}^{-2} \text{d}^{-1}$]
F_{p_0}	dispersive return flux to the overlying water [$\text{gP m}^{-2} \text{d}^{-1}$]
$F_{p_{2-3}}$	dispersive flux between two adjacent layers [$\text{gP m}^{-2} \text{d}^{-1}$]
$F_{pd_{2-3}}$	bioturbation flux between two adjacent layers [$\text{gP m}^{-2} \text{d}^{-1}$]
F_{ps_0}	seepage flux at the sediment-water interface [$\text{gP m}^{-2} \text{d}^{-1}$]
$F_{ps_{2-3}}$	seepage flux between two adjacent layers [$\text{gP m}^{-2} \text{d}^{-1}$]
F_{ps_4}	seepage flux at the lower boundary [$\text{gP m}^{-2} \text{d}^{-1}$]

Notice, that the resuspension of phosphate is taken into account explicitly, because of the importance for the phosphate budget in the overlying water. Phosphate adsorbed to resuspended sediments may desorb in the water column.

8 Silicate

Reactive silicate enters the sediment primarily in the form of opal silicate, the remains of diatom skeletons. Opal silicate dissolves gradually, because pore water is undersaturated with respect to silicate. The process is retarded by coating of the particles with minerals of iron and aluminum. Dissolved silicate may adsorb onto aluminum silicates and may precipitate in stable minerals (Berner, 1974; Vanderborght *et al.*, 1977a; Schink and Guinasso, 1978). Because all these processes are very slow and poorly understood, it was decided to include in SWITCH only the dissolution process.

Furthermore it is assumed that opal silicate is present in abundance in estuarine sediment. This seems a reasonable assumption considering the high productivity of diatoms and the slowness of the dissolution process. The rate is than only dependent on the difference between the saturation concentration and the actual dissolved concentration of silicate.

Sub-layers are not distinguished with respect to silicate. The mass balance of dissolved silicate in the pore water of the sediment is:

$$\frac{dCs_1}{dt} = (Fs_b - Fs_0 + Fss_0 - Fss_4)/(pa \cdot d) - ks \cdot (Cs_1 - Cs_s) \quad (8.1)$$

with:

$$pa = (p_1 \cdot dh + p_4 \cdot dl)/d$$

$$Fs_0 = 2pa \cdot D \cdot (Cs_1 - Cs_0)/(l + dh)$$

$$Fss_0 = -vs \cdot Cs_0 \quad \text{if } vs < 0 \cdot 0$$

$$Fss_4 = -vs \cdot Cs_1$$

$$Fss_0 = -vs \cdot Cs_1 \quad \text{if } vs > 0 \cdot 0$$

$$Fss_4 = -vs \cdot Cs_5$$

in which:

Cs_1	dissolved silicate concentration [gSi m^{-3}]
Cs_5	dissolved silicate concentration in the lower boundary layer [gSi m^{-3}]
Cs_s	saturation dissolved silicate concentration [gSi m^{-3}]
Fs_b	dissolution flux of opal silicate in the boundary layer [$\text{gSi m}^{-2} \text{d}^{-1}$]
Fs_0	dispersive return flux to the overlying water [$\text{gSi m}^{-2} \text{d}^{-1}$]
Fss_0	seepage flux at the sediment-water interface [$\text{gSi m}^{-2} \text{d}^{-1}$]
Fss_4	seepage flux at the lower boundary [$\text{gSi m}^{-2} \text{d}^{-1}$]
ks	dissolution rate [d^{-1}]
pa	average porosity [-]



DRAFT

9 Temperature dependency and dispersion

All process rates are temperature dependent according to:

$$k = k^{20}kt^{(T-20)} \quad (9.1)$$

in which:

k	first order process rate [d^{-1}]
k^{20}	first order process rate at 20 °C [d^{-1}]
kt	temperature coefficient [-]

Temperature coefficients may vary between 1.04 and 1.12.

Dispersion in the pore water is the result of molecular diffusion and bio-irrigation. The dispersion coefficient is defined as:

$$D = D_m + (bt - 1)D_m \quad (9.2)$$

in which:

D	dispersion coefficient [$m^2 d^{-1}$]
D_m	molecular diffusion coefficient [$m^2 d^{-1}$]
bt	amplification factor for bio-irrigation [-]

The amplification factor can be provided to the model as a sinus function with a period of one year and a maximum in the summer. The dispersion coefficient for bioturbation (D_b) can be assigned a similar function.

The dispersion coefficient at the water-sediment interface is multiplied with $(1-f_c)$, which reduces the dispersion flux according to the fraction of the surface area closed by mats of benthic algae.



DRAFT

References

- Berner, R., 1974. *The Sea: Marine Chemistry*, vol. 5, chap. Kinetic models for the early diagenesis of nitrogen, sulphur, phosphorus and silicon in anoxic marine sediments, pages 427–450. John Wiley & Sons, New York, pp.
- Brinkman, A. and W. van Raaphorst, 1986. *De fosfaathuishouding van het Veluwemeer*. Master's thesis, Twente University, The Netherlands. (in Dutch).
- Lijklema, L., 1980. "Interaction of ortho-phosphate with iron(III) and aluminum hydroxides." *Envir. Sci. Technol* 14: 537–541.
- Schink, D. and N. Guinasso, 1978. "Effects of bioturbation on sediment seawater interaction." *Mar. Geology* 23: 133–154.
- Smits, J. and D. Van der Molen, 1993. "Application of SWITCH, a model for sediment-water exchange of nutrients, to Lake Veluwe in the Netherlands." *Hydrobiologia* 253: 281–300.
- Van Raaphorst, W., P. Ruardij and A. Brinkman, 1988. *The Ecosystem of the Western Wadden Sea: Field Research and Mathematical modelling*, chap. The assessment of benthic phosphorus regeneration in an estuarine ecosystem model, pages 23–36. Netherlands Institute for Sea Research, Texel.
- Vanderborght, J., R. Wollast and G. Billen, 1977a. "Kinetic models of diagenesis in disturbed sediments: Part I. Mass transfer properties and silica diagenesis." *Limnol. Oceanogr* 22: 787–793.
- Vanderborght, J., R. Wollast and G. Billen, 1977b. "Kinetic models of diagenesis in disturbed sediments: Part II. Nitrogen diagenesis." *Limnol. Oceanogr* 22: 794–803.
- WL | Delft Hydraulics, 1991. *HADES; Ontwikkeling en verkennende berekeningen*. Research report T584, WL | Delft Hydraulics, Delft, The Netherlands. (in Dutch; N.M. de Rooij).
- WL | Delft Hydraulics, 1992. *Process formulations DBS*. Model documentation T542, WL | Delft Hydraulics, Delft, The Netherlands. (in Dutch; F.J. Los *et al.*).
- WL | Delft Hydraulics, 1994a. *Phosphate minerals in sediment: Literature study and analysis of field data*. Research report T584, WL | Delft Hydraulics, Delft, The Netherlands. (N.M. de Rooij and J.J.G. Zwolsman; in Dutch).
- WL | Delft Hydraulics, 1994b. *Switch, a model for sediment-water exchange of nutrients; Part 1: Formulation; Part 2: Calibration/Application for Lake Veluwe*. Research report T542/T584, WL | Delft Hydraulics, Delft, The Netherlands. (J.G.C. Smits).
- WL | Delft Hydraulics, 1994c. *SWITCH, a model for sediment-water exchange of nutrients. Part 3: Reformulation and recalibration for Lake Veluwe*. Research report T584, WL | Delft Hydraulics, Delft, The Netherlands. (J.G.C. Smits).
- WL | Delft Hydraulics, 1995. *Application DBS Lake Volkerak-Zoommeer, Phase 1*. Tech. Rep. T1440/T880, WL | Delft Hydraulics, Delft, The Netherlands. (in Dutch; B.F. Michielsen).
- WL | Delft Hydraulics, 1997. *Testing of DB-SWITCH regarding the applicability on peat lakes Geerplas and Nanneveld*. Research report T1697, WL | Delft Hydraulics, Delft, The Netherlands. (in Dutch; J.G.C. Smits).

DRAFT

DRAAFT



Photo by: Mathilde Matthijsse, www.zeelandonderwater.nl

Deltares **systems**

PO Box 177
2600 MH Delft
Rotterdamseweg 185
2629 HD Delft
The Netherlands

+31 (0)88 335 81 88
sales@deltaressystem.nl
www.deltaressystem.nl

